Utilisation of barium-modified analcime in sulphate removal: isotherms, kinetics and thermodynamics studies

Hanna Runtti[a], Pekka Tynjälä[b], Sari Tuomikoski*[a], Teija Kangas[a], Tao Hu[a], Jaakko Rämö[a] & Ulla Lassi[a,b]

[a]University of Oulu, Research Unit of Sustainable Chemistry, P.O.Box 3000, FI-90014 University of Oulu, Finland.

[b]University of Jyvaskyla, Kokkola University Consortium Chydenius, Unit of Applied Chemistry, Talonpojankatu 2B, FI-67100 Kokkola, Finland.

*Corresponding author: E-mail: sari.tuomikoski@oulu.fi; tel. +358 50 428 4057

Abstract

Analcime and commercial zeolite were employed as a precursor for preparing sorbent material for SO_4^{2-} removal over barium modification. Three sorbents were prepared: barium-modified analcime (ANA-Na-Ba), barium-modified acid-washed analcime (ANA-Ac-Na-Ba) and barium-modified zeolite (ZSM5-Na-Ba). Of the prepared materials, ANA-Ac-Na-Ba was the most efficient sorbent material for SO_4^{2-} removal, with a maximum sorption uptake of 13.7 mg g^{-1} at room temperature. Batch sorption experiments were performed to evaluate the effect of initial pH, initial SO_4^{2-} concentration, sorbent dosage, temperature and contact time of sorption. Several isotherms were applied to describe the experimental results and Bi-Langmuir was found to provide the best correlation for adsorption of SO_4^{2-} on ANA-Ac-Na-Ba. Kinetic studies were applied for the most effective sorbent material, ANA-Ac-Na-Ba, and the results showed that the sorption process follows pseudo-second-order kinetics.

Keywords: adsorption; sulphate; analcime; zeolite; chemical modification

1 Introduction

Natural zeolites are crystalline-hydrated "tectoaluminosilicate" minerals with cage-like structures [1,2]. Zeolites have a three-dimensional framework consisting of SiO_4 and AlO_4 tetrahedral molecules linked with shared oxygen atoms. Zeolites have a large surface area and high cation exchange capacity (CEC). The isomorphous replacement of Si^{4+} by Al^{3+} produces a negative charge, which is balanced by exchangeable alkali and alkaline-earth metal cations (Na^+, K^+, Ca^{2+} etc.). These cations are exchangeable with certain cations in solutions such as Pb^{2+}, Cd^{2+}, Zn^{2+} and Ni^{2+} [2]. Zeolites are usually pretreated with sodium solution before usage, because the ion exchange capacity of zeolite tends to increase if just monovalent cations are present in zeolite materials [3,4]. Zeolites can adsorb variably sized ions, which indicates their use as a selective adsorbent for many pollutants, including dyes [5,6], organics [7,8], ammonium [9,10] and metal ions [3,11] from wastewaters.

Zeolites can be found in volcanic environments (under hydrothermal conditions), salt lakes and sediment layers. The most common types of zeolites are clinoptilolite, mordenite, dachiardite, analcime (ANA), phillipsite and heulandite. Recently, ANA has also been reported to be an adsorbent in the wastewater treatment [12–14]. ANA ($NaAlSi_2O_6 \cdot H_2O$) is produced as a waste material in the mining industry, with irregular channels formed from four-, six- or eightfold rings [15]. Because zeolite materials have a low affinity for anions, chemical modification is needed to apply sorbent for anionic sulphate removal [2,16,17]. To remove anions from water, it is possible to modify natural zeolites with cationic surfactants (e.g. tetramethylammonium, hexadecyltrimethylammonium (HDTMA) bromide, tetrabutylammonium bromide (TBAB), n-cetylpyridinium bromide (CPB)) [1, 18-22]. Surface modification using cationic surfactant can change the surface charge and functionality by adding complex hydrophobic groups for positively charged exchange sites [2].

In addition, it is also possible to modify natural zeolites using inorganic salts (e.g. NaCl, $FeCl_3$, $BaCl_2$), which improves the sorption efficiency for anions [23,24]. The modification has been reported to create for example an oxi-hydroxide adsorption layer on the surface and change the surface charge from negative to positive [17,24]. Due to that, stable complexes with anions in solution are formed. In this study, the $BaCl_2$ modification was expected to impregnate Ba in the framework structure of zeolites and subsequently enable the surface precipitation or complexation of sulphate.

Sulphate (SO_4^{2-}) anion is a major pollutant that occurs in both natural waters and industrial effluent, such as acid mine drainage and wastes from the chemical industry [25,26]. SO_4^{2-} mainly results from the process of chemical weathering of sulphur-containing minerals (e.g. gypsum). In addition, SO_4^{2-} is generated through the oxidation of sulphides and elemental sulphur [27,28]. Sulphur is a necessary element for many kinds of organisms. However, excess SO_4^{2-} can cause an imbalance in the natural sulphur cycle [26–29]. In addition, SO_4^{2-} concentrations higher than 150 mg L^{-1} can damage water pipes [30] and concentrations higher than 600 mg L^{-1} can have laxative effects and affect the taste of the water [26].

SO_4^{2-} is common in drinking water and many countries have not set guidelines for it because it is only mildly hazardous [26,27]. In Finland, the SO_4^{2-} limit in drinking water is set at 250 mg L^{-1} [30]. Environmental agencies in many countries have set maximum SO_4^{2-} values of 250–1000 mg L^{-1} in both mine drainage and industrial effluent [26]. Typically, domestic sewage contains less than 500 mg L^{-1} of SO_4^{2-} but especially in industrial wastewater the concentration of SO_4^{2-} can be several thousand mg L^{-1} [29].

Some examples of established methods for the removal of SO_4^{2-} are chemical precipitation, biological treatment, ion exchange, reverse osmosis, electrodialysis and adsorption [26,28,31]. However, these methods suffered from various limitations. For example, biological treatment and ion exchange are expensive while precipitation (e.g. with lime) produces large amounts of sludge [26]. Furthermore, low SO_4^{2-} concentrations cannot be removed by lime precipitation

due to the high solubility of the produced $CaSO_4$ [32]. Among the various available water treatment technologies, adsorption may be preferred for SO_4^{2-} removal because it is a simple and effective technique. In addition, adsorption can be used in a so-called hybrid system with precipitation in which sulphate remaining after precipitation can be removed via adsorption. The success of this technique largely depends on the development of an efficient adsorbent [28,29,31]. Activated carbon [33], clay minerals [28,31], biomaterials [27,29], zeolites [35] and some industrial solid wastes [36] have been reported as adsorbents for SO_4^{2-} removal. However, there is still a need for alternative and locally available raw materials or industrial by-products with which to make sorbents.

The aim of this study was to investigate the effect of modification of natural analcime (ANA) to the sorption capacity for SO_4^{2-} removal from an aqueous solution. Commercial zeolite (ZSM5) was used as a reference material. Batch sorption experiments were performed to evaluate the influence of initial pH, initial SO_4^{2-} concentration, sorbent dosage, temperature and contact time. The Langmuir, Freundlich, Dubinin-Raduschkevich, Temkin, Bi-Langmuir, Sips, Redlich-Peterson and Toth isotherm models were applied to the experimental data. Kinetic studies were performed using pseudo-first-order, pseudo-second-order and Elovich kinetic models.

2 Materials and methods

2.1 Materials

Analcime (ANA) was obtained from a Finnish mining company. Commercial zeolite (NH_4-ZSM-5, 30:1 SiO_2:Al_2O_3, CAS: 1318-02-1) was used as a reference material (Alfa Aesar). Before use, all materials were dried overnight at 110°C, crushed and sieved to obtain a particle diameter less than 150 µm and to ensure a uniform product quality. The barium used in the modification was $BaCl_2$. SO_4^{2-} ion stock solutions were prepared by dissolving of Na_2SO_4 (VWR 99.9 %) in MilliQ water to generate a concentration of 5 g L^{-1} and the mixture was diluted with distilled water when necessary.

2.2 Characterisation methods

X-ray diffraction (XRD, PanAnalytical Xpert Pro) analysis was done for the untreated analcime and zeolite samples to identify the mineral type. In addition, the produced sorbent materials were characterized by XRD. X-ray fluorescence (XRF, PanAnalytical Minipal 4) analysis was carried out to determine the chemical compositions of untreated samples. Fourier Transform Infrared Spectroscopy (FTIR) spectra of the sorbent were collected using a Perkin Elmer Spectrum One spectrometer equipped with an Attenuated Total Reflectance (ATR) unit. The specific surface areas, pore sizes and pore volumes of samples were determined from nitrogen adsorption desorption isotherms at the temperature of liquid nitrogen (-196 °C) using a Micromeritics ASAP 2020.

2.3 Preparation of sorbents

Modification of analcime and zeolite was performed using two different protocols. By the protocol 1, analcime and zeolite were treated with NaCl and after that with $BaCl_2$ [37]. In the protocol 2, analcime was acid (HCl) washed before NaCl and $BaCl_2$ treatment.

Protocol 1: Analcime and ZSM-5 (5 g) was mixed with 1 M NaCl solution (50 mL) for 24 h, rinsed with deionised water and dried at 105 °C to ensure that all ion exchange sites were in Na form. The barium modification was done by mixing the material (5 g) with 1 M $BaCl_2$ solution (100 mL) for 16 h, rinsing with deionised water and drying at 105 °C. The materials were stored in a desiccator prior to use.

Protocol 2: Analcime (5 g) was acid washed with 2 M HCl (100 mL) for 24 h, rinsed with deionised water and dried 105 °C. Next, the analcime was mixed with 2 M NaCl solution (50 mL) for 24 h, rinsed with deionised water and dried at 105 °C to ensure that all ion exchange sites were in Na form. The barium modification was done by mixing the material (5 g) with 1 M $BaCl_2$ solution (100 mL) for 16 h, rinsing with deionised water and drying at 105 °C. The materials were stored in a desiccator prior to use.

2.4 Batch sorption experiments

In the sorption experiments, the effects of initial pH, initial SO_4^{2-} concentration, sorbent dosage, temperature and contact time on the removal efficiency of SO_4^{2-} over Ba-modified analcime (ANA-Na-Ba), Ba-modified acid-washed analcime (ANA-Ac-Na-Ba) and Ba-modified commercial zeolite (ZSM5-Na-Ba) were studied. The observed sorption conditions are presented in Table 1. Kinetic studies were performed in a 1 L reactor vessel equipped with a magnetic stirrer with an agitation speed of 1000 rpm.

Table 1. Parameters for testing the effects of initial pH, initial SO_4^{2-} concentration, sorbent dosage, contact time and temperature on SO_4^{2-} removal from synthetic solution.

Parameter	Sorbent	Initial pH	C_0 [mg L^{-1}]	Sorbent dosage [g L^{-1}]	Contact time	Temperature [°C]
Effect of initial pH	ANA-Na-Ba, ANA-Ac-Na-Ba, ZSM5-Na-Ba	2,4,6,8,10	100	5	24 h	23
Effect of initial SO_4^{2-} concentration	ANA-Na-Ba	5–7	10–1000	5	3 h	10,23,40
	ANA-Ac-Na-Ba	3–4				
	ZSM5-Na-Ba	4–7				
Effect of sorbent dosage	ANA-Na-Ba	5–7	100	1–25	2 h	10,23,40
	ANA-Ac-Na-Ba	3–4				
	ZSM5-Na-Ba	4–7				
Effect of contact time	ANA-Ac-Na-Ba	3–4	100	5	1 min – 24 h	23

ANA-Na-Ba: Barium-modified analcime, ANA-Ac-Na-Ba: Barium-modified acid-washed analcime, ZSM5-Na-Ba: Barium-modified commercial zeolite.

All sorption experiments were done duplicated. All samples were filtered through 0.45 μm filter paper (Sartorius Stedim Biotech) or separated using a centrifuge (3500 rpm, 5–15 min) before measurement of sulphate concentration by ion chromatography (Methrom 761 Compact IC).

2.5 Adsorption isotherms

Adsorption isotherms reveal the nature of the adsorption at varying initial concentrations in pH found to be optimal. The Langmuir, Freundlich, Dubinin-Raduschkevich, Temkin, Bi-Langmuir, Sips, Redlich–Peterson and Toth isotherm models were applied to the experimental data. Isotherm parameters were obtained using nonlinear regression with the Microsoft Excel (GRG nonlinear) solver tool.

The general non-linear form of Langmuir's [38] equation is

$$q_e = \frac{b_L q_m C_e}{1+b_L C_e}, \quad (3)$$

where q_e (mg g^{-1}) is the equilibrium adsorption capacity, q_m (mg g^{-1}) is the maximum adsorption capacity of the adsorbent and b_L (L mg^{-1}) is a constant related to the adsorption energy [39].

The Freundlich [40] model can be written as

$$q_e = K_F C_e^{1/n_F}, \quad (4)$$

where K_F (L mg^{-1}) is a relative indicator of adsorption capacity and dimensionless $1/n_F$ is the measure of surface heterogeneity, which becomes more heterogeneous as the value gets closer to zero [39].

The non-linear expression of the Dubinin-Radushkevich (D-R) isotherm model [41] can be illustrated as Eqs. 5 and 6:

$$q_e = {q_m}^{(-\beta\varepsilon^2)}, \quad (5)$$

$$\varepsilon = RTln\left(1 + \frac{1}{C_e}\right), \quad (6)$$

where β ($mol^2\ J^{-2}$) is a constant related to the mean free energy of adsorption per mole of the ion and ε is the Polanyi potential. R, T and C_e represent the gas constant (8.314 J $mol^{-1}\ K^{-1}$), absolute temperature (K) and adsorbate equilibrium concentration (mg L^{-1}), respectively [42].

The non-linear form of the Temkin isotherm [43] can be expressed by Eq. 7:

$$q_e = BlnA_TC_e, \quad (7)$$

where $B = (RT)/b_T$ is the Temkin constant related to the heat of the adsorption (J mol^{-1}), R (J mol^{-1} K^{-1}) is the gas constant, T(K) is the temperature, b_T is the Temkin isotherm constant and A_T (L g^{-1}) is the Temkin isotherm equilibrium binding constant [44].

The Bi-Langmuir isotherm [45] is presented in Eq. 8:

$$q_e = \frac{q_{m_1} b_{L_1} C_e}{1+b_{L_1} C_e} + \frac{q_{m_2} b_{L_2} C_e}{1+b_{L_2} C_e}, \quad (8)$$

where q_{m1} and q_{m2} are the maximum adsorption capacities (mg g^{-1}) of two different adsorption sites. Similarly, b_{L1} and b_{L2} (mg g^{-1}) represent the energies of adsorption at these sites [46,47].

The Sips isotherm [48] is given as

$$q_e = \frac{q_m (b_S C_e)^{n_S}}{1+(b_S C_e)^{n_S}}, \quad (9)$$

where b_S (L mg^{-1}) is a constant related to the adsorption energy and n_s is a dimensionless constant characterising the heterogeneity of the system [49].

Redlich–Peterson (R–P) isotherm [50] can be calculated from Eq. 10:

$$q_e = \frac{K_R C_e}{1+a_R C_e^{\beta}}, \quad (10)$$

where K_R (dm^3 g^{-1}) and a_R (dm^3 mg^{-1}) are R–P isotherm constants and β is an exponent, the value of which lies between 0 and 1. For β = 1, the equation reduces to the Langmuir equation, with

$a_R = b_L$. At high adsorbate concentrations, the equation is transformed into the Freundlich isotherm equation with $K_F = K_R/a_R$ and $1/n = 1-\beta$ [49, 51–54].

The Toth isotherm equation [55] can be written as in Eq. 11:

$$q_e = \frac{q_m K_{Th} C_e}{\left[1+(K_{Th}C_e)^{Th}\right]^{1/Th}}, \quad (11)$$

where K_{Th} (mg dm^{-3}) is the Toth isotherm constant and *Th* is the dimensionless Toth isotherm exponent, which characterises the heterogeneity of the system and is usually less than the unity. The more *Th* deviates from the unity, the larger is the heterogeneity of the adsorbent. When *Th* = 1, the Toth isotherm reduces to the Langmuir equation [51].

To evaluate the fit of the isotherm equations to the experimental data, the residual root mean square error (RMSE) and the chi-square test ($\chi 2$) were used. The smaller the error function value, the better the curve fitting. The calculated expressions of error functions can be defined as follows:

$$\text{RMSE} = \sqrt{\frac{1}{n-p}\sum_{i=1}^{n}(q_{e(\exp)} - q_{e(calc)})^2}, \quad (12)$$

$$\chi^2 = \sum_{n=1}^{n}\frac{(q_{e(exp)}-q_{e(calc)})^2}{q_{e(calc)}}, \quad (13)$$

where *n* is the number of experimental data, *p* is the number of parameters and $q_{e(exp)}$ and $q_{e(calc)}$ are the experimental and calculated values, respectively, of adsorption capacity in equilibrium [44,56,57].

2.6 Kinetic modelling

The kinetics of the adsorption experiments was investigated by applying the experimental data to pseudo-first-order, pseudo-second-order and Elovich models. The pseudo-first-order equation [58] is

$$log(q_e - q_t) = logq_e - \frac{k_f}{2.303}t, \quad (14)$$

where q_e (mg g^{-1}) and q_t (mg g^{-1}) are the amounts of ions adsorbed at equilibrium and at time t (min), respectively. k_f (min^{-1}) is the pseudo-first-order rate constant.

The linear form of the pseudo-second-order equation [59] is

$$\frac{t}{q_t} = \frac{1}{k_s q_e^2} + \frac{1}{q_e}t, \quad (15)$$

where k_s is the pseudo-second-order rate equilibrium constant (g mg^{-1} min^{-1}). The linear form of the Elovich equation from Zeldowitsch [60] is

$$q = \frac{1}{\beta}\ln\left(\upsilon_0\beta + \frac{1}{\beta}lnt\right), \quad (16)$$

where υ_0 (mg g^{-1} min^{-1}) is the initial adsorption rate and β (g mg^{-1}) is the desorption constant [61,62].

2.7 Thermodynamics of sorption

Thermodynamic constants including enthalpy change (ΔH), free energy change (ΔG) and entropy change (ΔS) were calculated using Eqs. 17–19.

$$\Delta G = -RTln(K), \quad (17)$$

$$K = \frac{q}{c_e}, \quad (18)$$

$$\ln K = \frac{\Delta S}{R} - \frac{\Delta H}{RT}, \quad (19)$$

where *ΔG* is the free energy change (kJ mol-1), *ΔH* is the change in enthalpy (kJ mol^{-1}), *ΔS* is the entropy change (kJ mol^{-1} K^{-1}), *T* is the absolute temperature (K) and *R* is the universal gas constant (8.314 J mol^{-1} K^{-1}) [51,63].

3 Results and discussion

3.1 Characterisation of the adsorbents

Chemical and mineral compositions of analcime (ANA) and commercial zeolite (ZSM-5) are presented in Table 2. The main chemical constituents of the ANA are SiO_2 (46.55%), Al_2O_3 (19.31%) and Na_2O (9.66%) whereas ZSM-5 consists mainly of SiO_2 (77.43%) and Al_2O_3 (4.35%). In addition, sorbents include some impurities and volatile compounds (e.g. water). According to the results, Si/Al ratio of analcime is about 2.0, which is similar for the analcimes reported by Atta *et al.* (2012) [12], Mallah *et al*. (2012) [13] and Liu *et al.* (2005) [64]. Si/Al ratio of commercial zeolite (ZSM-5, CAS: 1318-02-1) is 15, which is similar with the XRF result.

Table 2. Main chemical constituents of analcime (ANA) and zeolite (ZSM-5) as determined by XRF.

Composition	ANA [w/w%]	ZSM-5 [w/w%]
SiO_2	46.55	77.43
Al_2O_3	19.31	4.35
Na_2O	9.66	-
Fe_2O_3	1.25	0.04
K_2O	0.45	0.001
CaO	0.38	0.02
Others[a]	0.23	0.05
LOI[b]	9.00	7.20

[a]Including Mn, Ti, Zn, Bi, Rb, Ga, Ni, Cr etc. [b]Loss on ignition (at 950 °C).

The XRD patterns of ANA, ANA-Na-Ba, ANA-Ac-Na-Ba, ZSM-5 and ZSM5-Na-Ba are shown in Fig. 1. The XRD patterns of ANA and ANA-Na-Ba indicate the presence of sodium aluminum silicon oxide hydrate (analcime, $Na_8Al_8Si_{16}O_{48}(H_2O)_8$, JCPDS 04-009-3254) and silicon oxide (quartz, SiO_2, 01-070-3755). In addition, they might also contain lithium aluminum silicate (spodumene, $LiAlSi_2O_6$, 00-035-0797). The XRD pattern for commercial zeolite (ZSM-5, ammonium treated) indicate the structure of hydrogen aluminum silicate hydrate ($H_{6.9}Al_{6.9}Si_{89.1}O_{192}(H_2O)_{38}$, 04-013-2411). As can be seen from Fig. 1, it seems that barium modification did not change the chemical structure of ANA and ZSM-5. However, acid washing and further barium modification changed the structure of ANA. Acid treatment is generally employed to oxidise the surface of adsorbent, and it increases the acidity, removes the mineral elements and improves the hydrophilic nature of the surface [2]. Fig 1 shows that acid treatment analcime (ANA-Ac-Na-Ba) might also exhibit barium silicon aluminum oxide hydrate (edingtonite, $Ba_{0.89}(Si_{3.04}Al_{1,96})O_{10}(H_2O)_{3.32}$, 01-075-4005). However, it is quite difficult to distinguish edingtonite with spodumene, because the highest peak of edingtonite (211), 2θ of 25.4° is overlapped with spodumene (201), 2θ of 25.5°.

XRD results support results in Table 3. Barium modification has no significant effect on surface area, pore sizes, and volumes. However, the surface area and pore volumes clearly increase as a result of acid treatment and further barium modification in the case of analcime. In the literature, it has been reported that acid treatment increases the specific surface area and microporosity and reduces the cation-exchange capacity. This is due to that acid treatment can remove impurities that block the pores, progressively eliminate cations into H-form and finally dealuminate the structure [2,65,66].

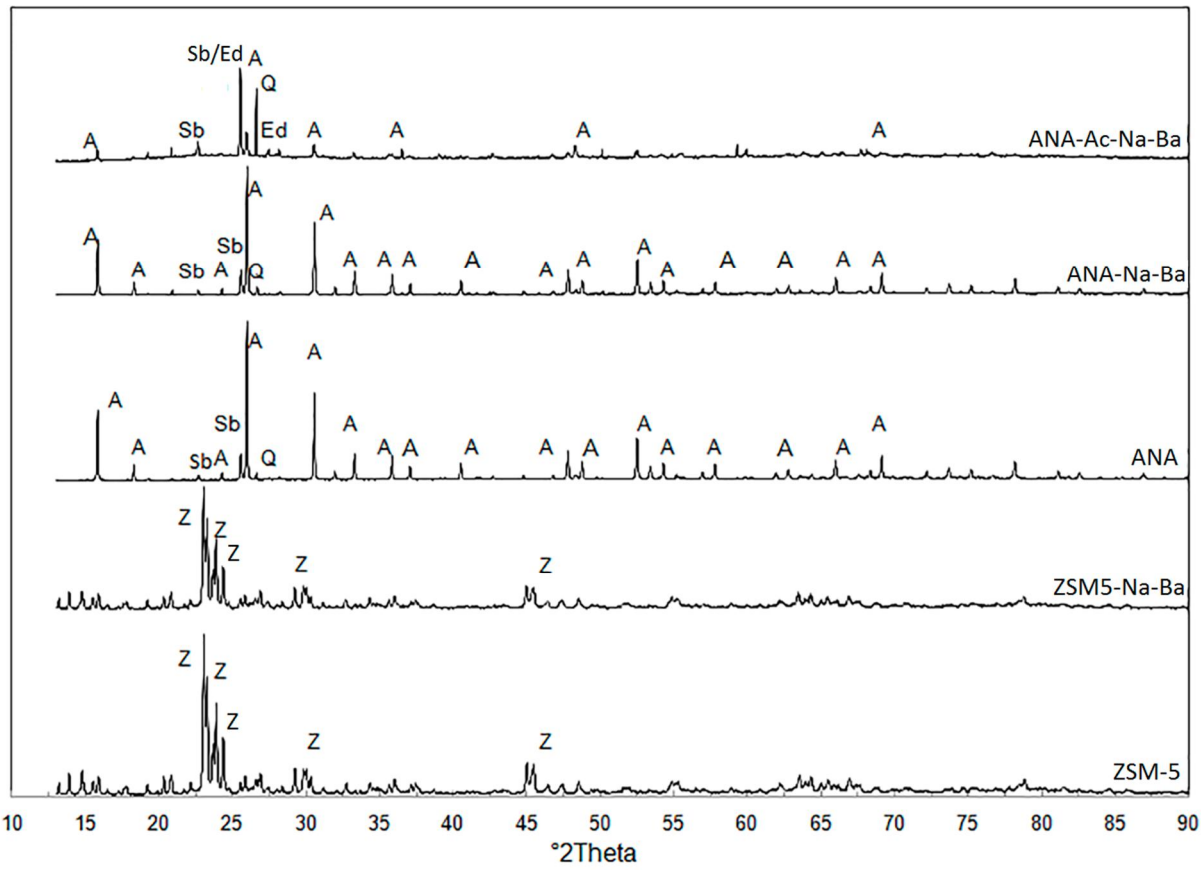

Figure 1. X-ray diffraction patterns of ANA-Ac-Na-Ba, ANA-Na-Ba, ANA, ZSM5-Na-Ba and ZSM-5. A: Analcime, Sb: Spodumene, Ed: Edingtonite, Q: Quartz, Z: Zeolite.

Table 3. Surface areas and pore volumes of raw materials (analcime and commercial zeolite) and modified zeolite materials.

Sorbent	Specific surface area [$m^2\ g^{-1}$]	$V_{macro+meso}$ [$cm^3\ g^{-1}$]	V_{micro} [$cm^3\ g^{-1}$]	V_{total} [$cm^3\ g^{-1}$]	Pore size [average, nm]
ANA	3.01	0.007	0.0003	0.008	9.99

ANA-Na-Ba	2.27	0.008	0.0002	0.009	15.17
ANA-Ac-Na-Ba	238.42	0.133	0.034	0.160	2.68
ZSM-5	321.61	0.252	0.022	0.274	3.41
ZSM5-Na-Ba	327.72	0.259	0.026	0.285	3.48

The FT-IR spectra of ANA, ANA-Na-Ba, ANA-Ac-Na-Ba, ZSM-5 and ZSM5-Na-Ba are shown in Fig. 2. The bands at 1632–1636 cm^{-1} are associated with water in the structure of the analcime and zeolite materials. The bands in the spectra of the materials appearing between 979–1086 cm^{-1} are related to the internal, anti-symmetric T–O (T = Al, Si) vibrations in tetrahedra or alumino- and silico-oxygen bridges. The bands between 739 and 803 cm^{-1} belong to T–O (T = Al, Si) symmetric stretching vibrations [1,15,67,68].

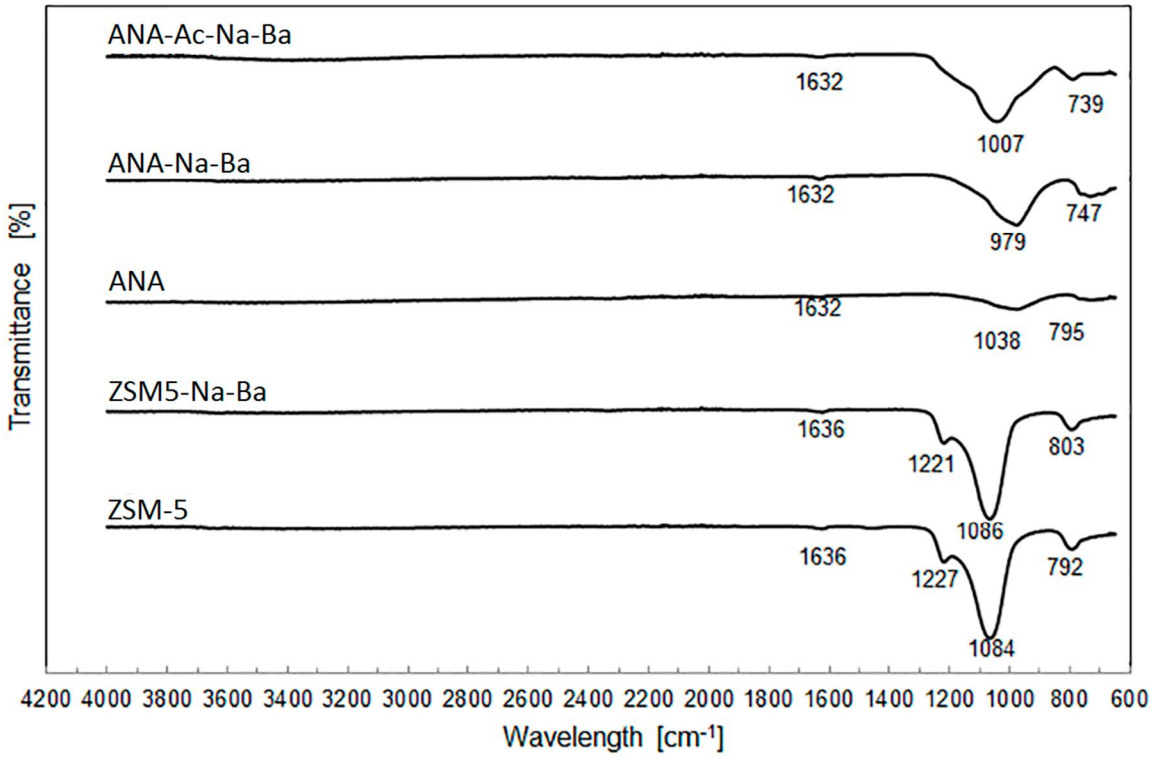

Figure 2. FT-IR spectrum of ANA-Ac-Na-Ba, ANA-Na-Ba, ANA, ZSM5-Na-Ba and ZSM-5.

3.2 Effect of initial pH

First, the effect of initial pH in the range of 2–10 was studied for the produced sorbents. The SO_4^{2-} ion removal efficiencies of the studied samples are shown in Fig. 3. In all cases, the sorption capacity starts to slowly decrease after the initial pH value exceeds 6. Especially in the case of ANA-Ac-Na-Ba removal, efficiency is better when the initial pH is lower than or equal to 6. The most probable reason for better removal under acidic conditions is the highly-protonated surface of sorbents in an acidic medium, which tends to adsorb negative ions. In addition, the large amount of OH^- competes with the SO_4^{2-} for unoccupied surface sites at a higher pH, which decreases the sorption of SO_4^{2-} [28,51,69,70]. In further experiments of this paper, initial pH

values for ANA-Na-Ba, ANA-Ac-Na-Ba, and ZSM5-Na-Ba were in the ranges of 5–7, 3–4, and 4–7, respectively. These pH ranges were optimal for maximum sulphate removal (Fig. 3). For ANA-Ac-Na-Ba, the initial pH was adjusted to 3–4 because pH increased one or two units during the adsorption experiment.

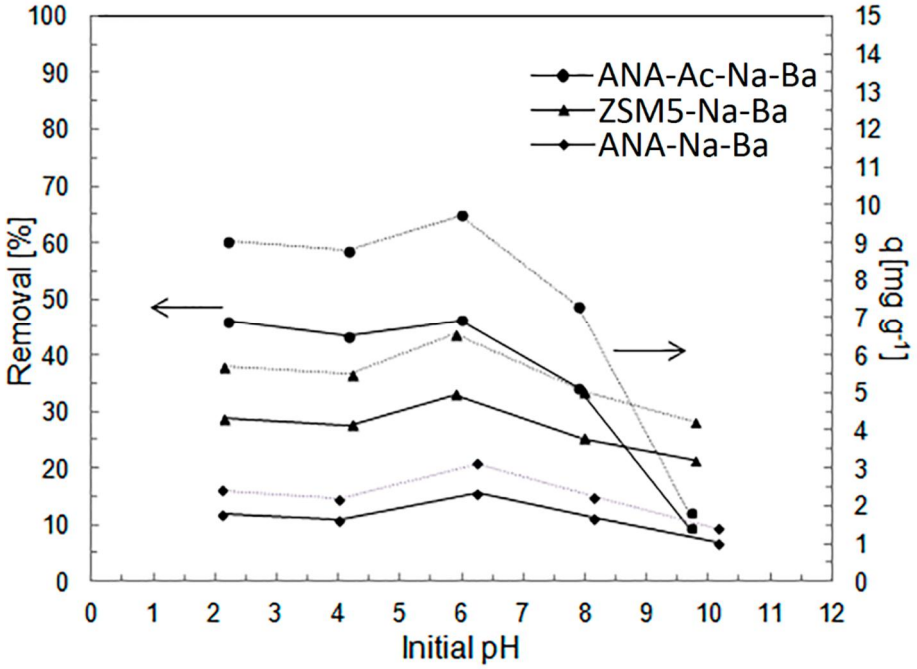

Figure 3. Total SO_4^{2-} removal per cent (left, solid lines) and total adsorbed amount (right, dashed lines) versus initial pH on the sorption of SO_4^{2-} onto ANA-Na-Ba, ANA-Ac-Na-Ba and ZSM5-Na-Ba. Sorbent dose: 5 g L^{-1}, $C_0(SO_4^{2-})$: 100 mg L^{-1}, contact time: 24 h, temperature: 22–23 °C.

3.3 Effect of sorbent dose

The effect of ANA-Na-Ba, ANA-Ac-Na-Ba and ZSM5-Na-Ba dose on the sorption of SO_4^{2-} at different temperatures (10, 23, 40 °C) is shown in Fig. 4. The sorption capacities (q_e) decrease when the sorbent dose increases (dashed lines in Fig. 4), which can be explained by the increase

in the sorbent to adsorbate ratio. The higher the dosage, the greater the number of available adsorption sites there are against the SO_4^{2-} ions. This leads to the unsaturation of the sorption sites and results in comparatively less sorption amount at a higher sorbent dosage. The differences between sorption capacities at different temperatures are very minor, but it seems that sorption is more efficient at higher temperatures in all cases [51, 71–73].

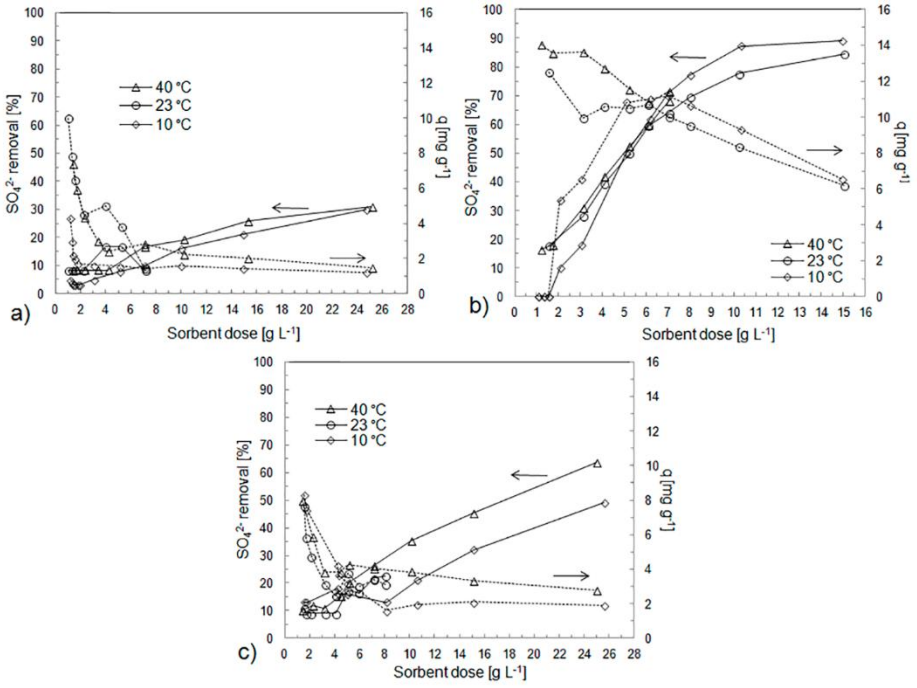

Figure 4. Effect of sorbent dosage on SO_4^{2-} removal at different temperatures (10, 23, 40 °C). a) ANA-Na-Ba, initial pH: 5–7; b) ANA-Ac-Na-Ba, initial pH: 3–4; and c) ZSM5-Na-Ba, initial pH: 4–7. Removal % of SO_4^{2-} is marked with a solid line, and sorption capacities (q) are marked with a dashed line. In all cases, $C_0(SO_4^{2-})$: ~100 mg L-1, contact time: 3 h and temperature: 22–23 °C.

3.4 Effect of initial SO_4^{2-} concentration

The effect of SO_4^{2-} concentration was studied at three temperatures. The SO_4^{2-} uptake mechanism is particularly dependent on the initial SO_4^{2-} concentration: at low concentrations, SO_4^{2-} are sorbed by specific sites, while with increasing SO_4^{2-} concentrations the specific sites are saturated and the exchange sites are filled [69,70]. In the case of SO_4^{2-} removal by ANA-Na-Ba at 10 and 40 °C, removal efficiency (%) increases as initial concentration increases but then starts to decrease. This phenomenon occurs due to the increased of a driving force provided by the concentration gradient when the initial SO_4^{2-} concentration in the solution is increased [69]. The sorption capacities (q, mg g^{-1}) and removal efficiencies (%) increase as temperature is increased. The same phenomenon has been seen in sorbent dose optimisation studies. This indicates that sorption is an endothermic in nature. However, differences between sorption capacities and removal efficiencies at different temperatures are minor, especially at low initial concentrations. The probable removal mechanism of SO_4^{2-} on the zeolite materials is based on the surface complexation or precipitation of extremely low solubility of $BaSO_4$ [2,17]. Fig. 5 shows the effect of SO_4^{2-} concentration on the removal and sorption capacity of SO_4^{2-} at these temperatures.

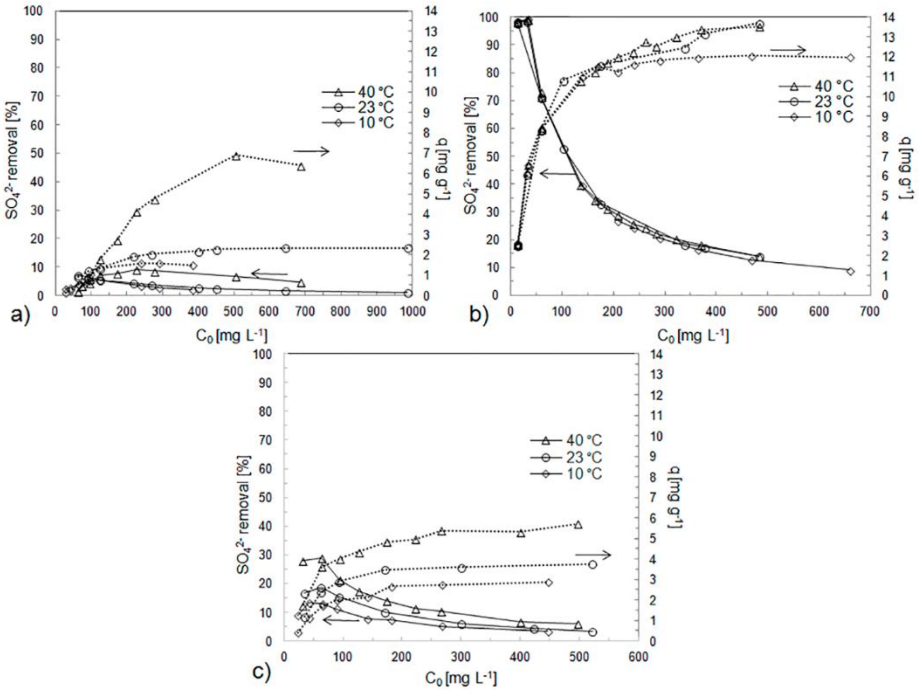

Figure 5. Effect of initial concentration on SO_4^{2-} removal at different temperatures (10, 23, 40 °C). a) ANA-Na-Ba, initial pH: 5–7; b) ANA-Ac-Na-Ba, initial pH: 3–4; and c) ZSM5-Na-Ba, initial pH: 4–7. Removal % of SO_4^{2-} is marked with a solid line, and sorption capacities (q) are marked with a dashed line. In all cases, sorbent dosage: 5 g L^{-1} and contact time: 2 h.

3.5 Adsorption isotherms

Langmuir, Freundlich, D-R, Temkin, Bi-Langmuir, Sips, R-P and Toth isotherm models were applied for the experimental results of ANA-Na-Ba, ANA-Ac-Na-Ba and ZSM5-Na-Ba. Isotherm parameters, errors and graphs are shown in supplementary material. Comparison of the errors (RMSE, χ^2) and correlation coefficients (R^2) indicated that the SO_4^{2-} sorption onto ANA-Na-Ba and ZSM5-Na-Ba can be best represented by the Sips model at the temperatures 10 and 40°C while the R–P and Sips models were favourable at 23°C. This is logical result because Sips model is known to be applicable to the porous materials. In the case of ANA-Ac-Na-Ba, Bi-Langmuir

showed the best fit at all studied temperatures, which indicates monolayer adsorption to two kind of sorption sites. The difference between the indicating values of the models was relatively small when best models were compared. However, differences were quite large between the best and the worst models. The maximum experimental sorption capacities were 2.3, 13.7 and 3.8 mg g^{-1} for ANA-Na-Ba, ANA-Ac-Na-Ba and ZSM5-Na-Ba, respectively, at room temperature. ANA-Ac-Na-Ba was the best sorbent and it was compared with sorbents reported in other studies (Table 4). The adsorption capacities of the barium-modified acid-washed analcime (ANA-Ac-Na-Ba) in SO_4^{2-} removal are comparable with values presented in the literature.

Table 4. Comparison of adsorption capacity q_m(mg g^{-1}) of various sorbents for the removal of SO_4^{2-} from aqueous phase.

Sorbent	Capacity q [mg g^{-1}]	Initial pH	C_0 [mg L^{-1}]	Sorbent dose [g L^{-1}]	Time [h/min]	T [°C]	Ref.
Surfactant-modified palygorskite	3.24[a]	4	20–130[c]	10	4 h	35	[28]
$ZnCl_2$ activated coir pith carbon	4.9[a]	4	20–80[c]	10	30 min	35	[74]
Surfactant-modified clinoptilolite	~ 7.0[a]	4.0–5.1	96–500[c]	-	8 h	25	[35]
ɣ-Al_2O_3	7.7	5.7	20-40[c]	-	24 h	25	[75]
Surfactant-modified coir pith	8.76[a]	2	10–50[c]	4	-	32	[29]
Raw rice straw	11.68[a]	6.4	50–500 [c]	2	2 h	25	[27]
Barium-modified acid-washed analcime	13.7[b]	3–6	10–500 [c]	5	2 h	20–23	*This study*
Limestone	23.7[a]	9.6-9.8	588–3000[d]	25	9 h	23	[26]
Alkali-treated fly ash	43[a]	-	200[e]	-	~ 4 h	-	[76]
Epichlorohydrin and trimethylamine modified rice straw	74.76[a]	6.4	50–500[c]	2	2 h	25	[27]
Poly(*m*-phenylenediamine)	108.5[a]	1.75	500–4000[c]	-	1 h	23	[31]
Ba-modified blast furnace-slag geopolymer	119[b]	7–8	865[d]	5	24	20–23	[37]
Chitin-based shrimp shells	156.0[a]	4.3	2350[c]	10	1 h	-	[77]

[a]Langmuir maximum sorption capacity, $q_{m,calc}$. [b]Experimental maximum sorption capacity, $q_{m,exp}$. [c]Synthetic [d]Mine effluent, [e]Ground water.

3.6 Kinetic modelling

Kinetic modeling was performed only for the best sorbent, ANA-Ac-Na-Ba, at room temperature. Sorption equilibrium was attained at approximately 1 min, and it remained constant thereafter. Maximum SO_4^{2-} removal and sorption capacity were 99.1% and 6.3 mg g^{-1} (Fig not shown). Pseudo-first-order, pseudo-second-order and Elovich models were applied to the experimental data. Fits are shown in Fig. 6, and the corresponding kinetic parameters and correlation coefficients are presented in Table 4. The correlation coefficient (R^2) of the pseudo-second-order model was clearly higher than the R^2 values of the pseudo-first-order and Elovich models. In addition, the experimental sorption capacity ($q_{e,exp}$) of the pseudo-second-order model agrees with the calculated sorption capacity ($q_{e,calc}$), which means that the sorption of SO_4^{2-} ions onto ANA-Ac-Na-Ba follows the pseudo-second-order kinetic model. This indicates that the rate of the adsorption process depends on the amount of SO_4^{2-} and available adsorption sites.

Table 5. Pseudo-first-order, pseudo-second-order and Elovich model parameters for ANA-Ac-Na-Ba in SO_4^{2-} removal.

Experimental/Model	Constant [Unit]	Value
Experimental	Removal [%]	98.1
	$q_{e(exp)}$[mg g^{-1}]	6.34
Pseudo-first-order	$q_{e(cal)}$ [mg g^{-1}]	0.08
	k_1 [min^{-1}]	0.009
	R^2	0.757
Pseudo-second-order	$q_{e(cal)}$ [mg g^{-1}]	6.35
	k_2 [g $mg^{-1}min^{-1}$]	0.406
	R^2	1
Elovich	β [g mg^{-1}]	62.893
	υ_0[mg g^{-1} min^{-1}]	2.4E+168
	R^2	0.756

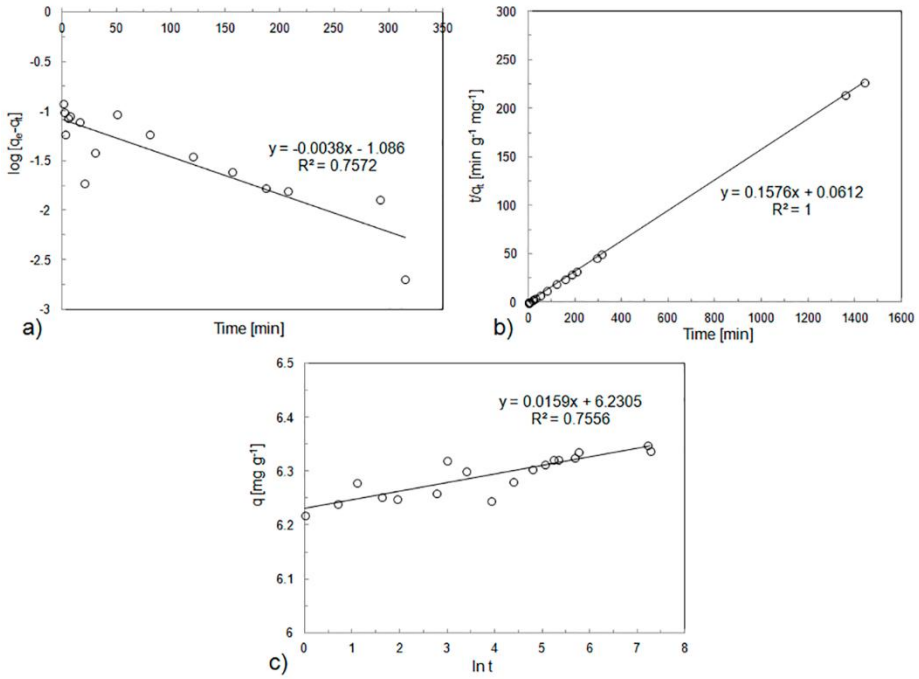

Figure 6. a) Pseudo-first-order, b) pseudo-second-order and c) Elovich model plots of SO_4^{2-} removal ANA-Ac-Na-Ba. Adsorbate: model solution (C_0, SO_4^{2-}: 100 mg L^{-1}), initial pH: 3–4, sorbent dose: 5 g L^{-1}, contact time: 24 h, and temperature: 20–23 °C.

3.7 Effect of temperature

Effect of temperature was studied by performing the experiments in three different temperatures (10, 20, 40 °C). As can be seen in Fig. 4 the rise of temperature increases the removal efficiency (%). However, the effect is minor. *ΔH* and *ΔS* values were obtained from the slope and intercept of the plot of *ln Kc* vs. *1/T*, as shown in Fig. 7 and listed in Table 5. The negative values of *ΔG* indicated that the sorption process was spontaneous in nature. The reaction is more spontaneous in the higher temperatures. The affinity of the modified sorbent materials for SO_4^{2-} are represented by the positive values of *ΔS*, which indicates that the sorption process increased the randomness at the solid/solution interface during the sorption

process. The positive values of ΔH suggest that the interaction of SO_4^{2-} and ANA-Na-Ba, ANA-Ac-Na-Ba and ZSM5-Na-Ba is endothermic in nature. Because the ΔH values obtained in this study are lower than 40 kJ mol^{-1}, the type of sorption is likely a physical process, involving weak interactions [69, 70, 78–80].

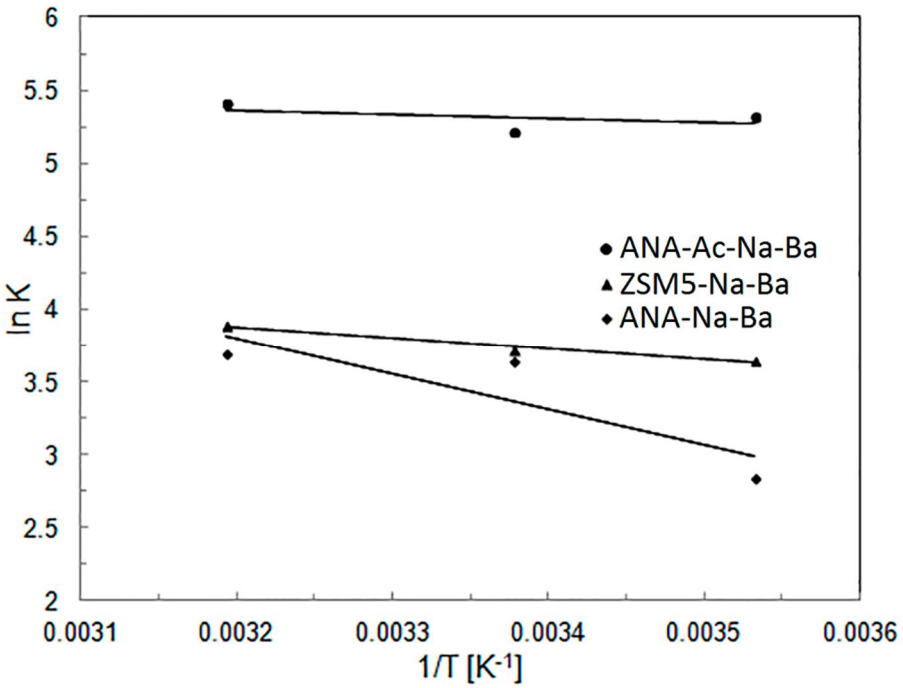

Figure 7. Van't Hoff plots for the adsorption of SO_4^{2-} removal. Conditions: sorbent dose: 5 g L^{-1}, initial pH: 5–7 (ANA-Na-Ba), 3–4 (ANA-Ac-Na-Ba), 4–7 (ZSM5-Na-Ba), initial concentration: 100 mg L^{-1}.

Table 6. Thermodynamic parameters for the sorption of SO_4^{2-} on ANA-Na-Ba, ANA-Ac-Na-Ba and ZSM5-Na-Ba at different temperatures.

Sorbent	Removal [%]			$q_{m,exp}$ [mg g^{-1}]			ΔG [kJ mol^{-1}]			ΔS [J mol^{-1} K^{-1}]	ΔH [kJ mol^{-1}]
	10°C	23°C	40°C	10°C	23°C	40°C	10°C	23°C	40°C		
ANA-Na-Ba[a]	8.0	16.7	17.5	1.6	3.8	3.9	-6.7	-9.0	-9.6	96.7	20.4
ANA-Ac-Na-Ba[b]	51.8	50.0	55.0	10.8	10.5	11.6	-12.5	-12.8	-14.1	51.8	2.3
ZSM5-Na-Ba[c]	16.0	17.3	20.0	3.2	3.8	4.3	-8.6	-9.2	-10.1	51.2	6.0

Initial pH: a) 5–7, b) 3–4, c) 4–7. In all cases, sorbent dose: 5 g L^{-1}, initial SO_4^{2-} concentration: 100 mg L^{-1}.

Conclusions

Ba-modified analcime with (ANA-Ac-Na-Ba) and without acid-washing (ANA-Na-Ba) and Ba-modified ZSM-5 (ZSM5-Na-Ba) were studied for SO_4^{2-} removal. ANA-Ac-Na-Ba was found to be the most effective adsorbent of these three sorbent materials. The removal efficiencies were better at higher temperatures, indicating that adsorption is an endothermic process. Several isotherm models were applied to generate the experimental results of all sorbents. According to the results SO_4^{2-} sorption onto ANA-Ac-Na-Ba from model SO_4^{2-} solution can be best represented by the Bi-Langmuir at 10, 23 and 40°C, which indicates monolayer adsorption to two different kind of adsorption sites.

The results from the present study indicate that Ba-modified acid-washed analcime could be a feasible SO_4^{2-} sorbent in wastewater treatment (e.g. mining industry). Compared with the

adsorption capacities of other sorbents developed for SO_4^{2-} removal, the results obtained in this study are in the same order of magnitude. Acid treatment and barium modification notably increases the adsorption capacity of SO_4^{2-} compared with untreated or barium-modified analcime.

Acknowledgments

This study has been undertaken with the financial support of the project SULKA (A32164, 524/2012) and Maa- ja vesitekniikan tuki ry. The authors would like to thank MSc Sara Lopéz and BSc Riikka Juhola for their contribution in some laboratory experiments. The authors would also like to thank Mr. Jaakko Pulkkinen and Mr. Tuomo Vähätiitto for their assistance in SO_4^{2-} ion analysis. Finally, the authors would like to thank Kai Tiihonen and Marjukka Hyyryläinen at the Kajaani University of Applied Sciences for their contribution to XRF measurements.

References

[1] K. Barczyk, W. Mozgawa, M. Król, Studies of anions sorption on natural zeolites, Spectrochim. Acta Part A: Molec. Biomolec. Spectrosc. 133 (2014) 876–882.

[2] S. Wang, Y. Peng, Natural zeolites as effective adsorbents in water and wastewater treatment, Chem. Eng. J. 156 (2010) 11–24.

[3] A. Cincotti, A. Mameli, A.M. Locci, R. Orru, G. Cao, Heavy metals uptake by Sardinian natural zeolites: Experiment and modeling. Ind. & Eng. Chem. Res. 45 (2006) 1074–1084.

[4] L.R. Weatherley, N.D. Miladinovic, Comparison of the ion exchange uptake of ammonium ion onto New Zealend clinoptilolite and mordenite, Water Res. 38 (2004) 4305–4312.

[5] D. Karadag, E. Akgul, S. Tok, F. Erturk, M.A. Kaya, M. Turan, Basic and reactive dye removal using natural and modified zeolites. J. Chem. Eng. Data 52 (2007) 2436–2441.

[6] S. Wang, Z.H. Zhu, Characterisation and environmental application of an Australian natural zeolite for basic dye removal from aqueous solution, J. Hazard. Mater. 136 (2006) 946–952.

[7] R.S. Bowman, Applications of surfactant–modified zeolites to environmental remediation, Micropor. Mesopor. Mat. 61 (2003) 43–56.

[8] P. Huttenloch, K.E. Roehl, K. Czurda, Sorption of nonpolar aromatic contaminants by chlorosilane surface modified natural minerals. Environ. Sci. Technol. 35 (2001) 4260–4264.

[9] L. Lei, X. Li, X. Zhang, Ammonium removal from aqueous solutions using microwave–treated natural Chinese zeolite, Sep. Purif. Technol. 58 (2008) 359–366.

[10] T. Luukkonen, M. Sarkkinen, K. Kemppainen, J. Rämö, U. Lassi, Metakaolin geopolymer characterization and application for ammonium removal from model solutions and landfill leachate, Appl. Clay. Sci. 119, Part 2 (2016) 266–276.

[11] O. Oter, H. Akcay, Use of natural clinoptilolite to improve, water quality: sorption and selectivity studies of lead(II), copper(II), zinc(II), and nickel(II). Water Environ. Res. 79 (2007) 329–335.

[12] A.Y. Atta, B.Y. Jibril, B.O. Aderemi, S.S. Adefila, Preparation of analcime from local kaolin and rice husk ash, Appl. Clay. Sci. 61 (2012) 8–13.

[13] M.H. Mallah, H. Soorchi, T.F. Jooybari, Development of empirical equation for analcime in the treatment of nuclear waste, Ann. Nucl. Energy. 47 (2012) 140–145.

[14] S. Montalvo, L. Guerrero, R. Borja, E. Sánchez, Z. Milán, I. Cortés, Angeles de la la Rubia,M., Application of natural zeolites in anaerobic digestion processes: A review, Appl. Clay. Sci. 58 (2012) 125–133.

[15] X. Ma, J. Yang, H. Ma, C. Liu, P. Zhang, Synthesis and characterization of analcime using quartz syenite powder by alkali–hydrothermal treatment, Micropor. Mesopor. Mat. 201 (2015) 134–140.

[16] S. Samatya, U. Yuksel, M. Yuksel & N. Kabay, Removal of fluoride from water by metal ions (Al^{3+}, La^{3+} and ZrO^{2+}) loaded natural zeolite. Sep. Sci. Technol. 42 (2007) 2033–2047.

[17] K. Margeta, N.Z. Logar, M. Šiljeg & A. Farkaš, Natural zeolites in water treatment– How effective is their use (2013), http://dx.doi.org/10.5772/50738.

[18] H. Faghihian, A. Mostafavi & A. Mohammadi, Surface modification of analcime for removal of nitrite and nitrate from aqueous solutions. J. Sci. I. Iran 12 (2001) 327–332.

[19] S. Sharafzadeha, A. Nezamzadeh-Ejhieh, Using of anionic adsorption property of a surfactant modified clinoptilolite nano-particles in modification of carbon paste electrode as effective ingredient for determination of anionic ascorbic acid species in presence of cationic dopamine species, Electrochim Acta 184 (2015) 371–380.

[20] A. Nezamzadeh-Ejhieh, A. Esmaeilian, Application of surfactant modified zeolite carbon paste electrode (SMZ-CPE) towards potentiometric determination of sulfate, Micropor Mesopor Mat 147 (2012) 302–309

[21] Z. Hoseini, A. Nezamzadeh-Ejhieh, An oxalate selective electrode based on modified PVC-membrane with tetra-butylammonium — Clinoptilolite nanoparticles, Mat. Sci. Eng. C 60 (2016) 119–125

[22] M. Ghiaci, R. Kia, A. Abbaspur & F. Seyedeyn-Azad, Adsorption of chromate by surfactant modified zeolites and MCM-41 molecular sieve. Sep. Purif. Technol. 40 (2004) 285–295.

[23] C.R. Oliveira, J. Rubio, New basis for adsorption of ionic pollutants onto modified zeolites,

Min. Eng. 20 (2007) 552–558.

[24] M. Šiljeg, Š. C. Stefanović, M. Mazaj, N. N. Tušar, I. Arčon, J. Kovač, K. Margeta, V. Kaučič, N. Z. Logar, Structure investigation of As(III)- and As(V)-species bound to Fe-modified clinoptilolite tuffs, Micropor. Mesopor. Mat. 118 (2009) 408–415.

[25] D.R. Mulinari, M.L.C.P. da Silva, Adsorption of sulphate ions by modification of sugarcane bagasse cellulose, Carbohydr. Polym. 74 (2008) 617–620.

[26] A.M. Silva, R.M.F. Lima, V.A. Leão, Mine water treatment with limestone for sulfate removal, J. Hazard. Mater. 221–222 (2012) 45–55.

[27] W. Cao, Z. Dang, X. Zhou, X. Yi, P. Wu, N. Zhu, G. Lu, Removal of sulphate from aqueous solution using modified rice straw: Preparation, characterization and adsorption performance, Carbohydr. Polym. 85 (2011) 571–577.

[28] D. Rui, L. Yuanfa, W. Xingguo, H. Jianhua, Adsorption of sulfate ions from aqueous solution by surfactant-modified palygorskite, J. Chem. Eng. Data. 56 (2011) 3890–3896.

[29] C. Namasivayam, M.V. Sureshkumar, Removal of sulfate from water and wastewater by surfactant-modified coir pith, an agricultural solid "waste" by adsorption methodology, J. Env. Eng. Manage. 17 (2007) 129–135.

[30] Finlex, Ministry of Social Affairs and Health, 1352/2015 Sosiaali- ja terveysministeriön asetus talousveden laatuvaatimuksista ja valvontatutkimuksista (In Finnish), http://www.finlex.fi, 2015 (accessed 01.12.15).

[31] P. Sang, Y. Wang, L. Zhang, L. Chai, H. Wang, Effective adsorption of sulfate ions with poly(m-phenylenediamine) in aqueous solution and its adsorption mechanism, Transactions of Nonferrous Metals Society of China. 23 (2013) 243–252.

[32] L. Hartinger, Handbook of effluent treatment and recycling for the metal finishing industry, 2. ed., ASM International, Novelty, OH, USA, 1994.

[33] M.S. Salman, Removal of sulfate from waste water by activated carbon, Al-Khwarizmi Eng. J. 5 (2009) 72–76.

[34] R.P.J.J. Rietra, T. Hiemstra, W.H. van Riemsdijk, Comparison of Selenate and Sulfate Adsorption on Goethite, J. Colloid Interface Sci. 240 (2001) 384–390.

[35] A.D. Vujaković, M.R. Tomašević-Čanović, A.S. Daković, V.T. Dondur, The adsorption of sulphate, hydrogenchromate and dihydrogenphosphate anions on surfactant-modified clinoptilolite, Appl. Clay. Sci. 17 (2000) 265–277.

[36] E. Iakovleva, E. Mäkilä, J. Salonen, M. Sitarz, M. Sillanpää, Industrial products and wastes as adsorbents for sulphate and chloride removal from synthetic alkaline solution and mine process water, Chem. Eng. J. 259 (2015) 364–371.

[37] H. Runtti, T. Luukkonen M. Niskanen, S. Tuomikoski, T. Kangas, P. Tynjälä E.-T. Tolonen, M. Sarkkinen, K. Kemppainen J. Rämö U. Lassi, Sulphate removal over barium-modified blast-furnace-slag geopolymer, J. Hazard. Mater. 317 (2016) 373–384.

[38] I. Langmuir, The adsorption of gases on plane surfaces of glass, mica and platinum. J. Am. Chem. Soc 40 (1918) 1361–1403.

[39] A. Bhatnagar, A.K. Minocha, M. Sillanpää, Adsorptive removal of cobalt from aqueous solution by utilizing lemon peel as biosorbent, Biochem. Eng. J. 48 (2010) 181–186.

[40] H.M.F. Freundlich, Over the adsorption in solutions. J. Phys. Chem. 57 (1918) 385–470.

[41] M.M. Dubinin, L.V. Radushkevich, The equation of the characteristic curve of the activated charcoal. Proc. Acad. Sci. USSR Phys. Chem. Sect. 55 (1947) 331–337.

[42] K.Y. Foo, B.H. Hameed, Insights into the modeling of adsorption isotherm systems, Chem. Eng. J. 156 (2010) 2–10.

[43] M.J. Temkin, V. Pyzhev, Recent modifications to Langmuir isotherms. Acta Physicochim URSS 12 (1940) 217–222.

[44] R. Rostamian, M. Najafi, A.A. Rafati, Synthesis and characterization of thiol-functionalized silica nano hollow sphere as a novel adsorbent for removal of poisonous heavy metal ions from water: Kinetics, isotherms and error analysis, Chem. Eng. J. 171 (2011) 1004–1011.

[45] D. Graham, The characterization of physical adsorption systems. I. the equilibrium function and standard free energy of adsorption. J. Phys. Chem. 57 (1953) 665–669.

[46] E. Repo, R. Petrus, M. Sillanpää, J.K. Warchol, Equilibrium studies on the adsorption of Co(II) and Ni(II) by modified silica gels: One-component and binary systems. Chem. Eng. J. 172 (2011) 376–385.

[47] E. Repo, T.A. Kurniawan, J.K. Warchol, M. Sillanpää, Removal of Co(II) and Ni(II) ions from contaminated water using silica gel functionalized with EDTA and/or DTPA as chelating agents. J. Hazard. Mater. 171 (2009) 1071–1080.

[48] R. Sips, On the structure of a catalyst surface. J. Chem. Phys. 16 (1948) 490–495.

[49] E. Salehi, S.S. Madaeni, F. Heidary, Dynamic adsorption of Ni(II) and Cd(II) ions from water using 8-hydroxyquinoline ligand immobilized PVDF membrane: isotherms, thermodynamics and kinetics. Sep. Purif. Technol. 94 (2012) 1–8

[50] O. Redlich, DL Peterson, A useful adsorption isotherm. J. Phys. Chem. 63 (1959) 1024–1024.

[51] D.H. Lataye, I.M. Mishra, I.D. Mall, Adsorption of α-picoline onto rice husk ash and granular activated carbon from aqueous solution: Equilibrium and thermodynamic study, Chem. Eng. J. 147 (2009) 139–149.

[52] A.C.A. de Lima, R.F. Nascimento, F.F. de Sousa, J.M. Filho, A.C. Oliveira, Modified coconut shell fibers: A green and economical sorbent for the removal of anions from aqueous solutions, Chem. Eng. J. 185–186 (2012) 274–284.

[53] M. Najafi, Y. Yousefi, A.A. Rafati, Synthesis, characterization and adsorption studies of several heavy metal ions on amino-functionalized silica nano hollow sphere and silica gel. Sep. Purif. Technol. 85 (2012) 193–205.

[54] C. Quintelas, Z. Rocha, B. Silva, B. Fonseca, H. Figueiredo, T. Tavares T, Removal of Cd(II), Cr(VI), Fe(III) and Ni(II) from aqueous solutions by an E. coli biofilm supported on kaolin. Chem. Eng. J. 149 (2009) 319–324.

[55] J. Toth, State equations of the solid gas interface layer, Acta Chem. Acad. Hung. 69 (1971) 311–328.

[56] O. Duman, S. Tunç, T.G. Polat, Determination of adsorptive properties of expanded vermiculite for the removal of C. I. Basic Red 9 from aqueous solution: Kinetic, isotherm and thermodynamic studies, Appl. Clay. Sci. 109–110 (2015) 22–32.

[57] R. Han, J. Zhang, P. Han, Y. Wang, Z. Zhao, M. Tang, Study of equilibrium, kinetic and thermodynamic parameters about methylene blue adsorption onto natural zeolite, Chem. Eng. J. 145 (2009) 496–504.

[58] S. Lagergren, About the theory of so-called adsorption of soluble substances., K. Sven. Vetenskapsakad. Handl. 24 (1898) 1–39.

[59] Y.S. Ho, G. McKay, Pseudo-second order model for sorption processes, Process Biochem. 34 (1999) 451–465.

[60] J. Zeldowitsch, Über den mechanismus der katalytischen oxydation von CO an MnO_2 [About the mechanism of catalytic oxidation of CO over MnO_2], Acta Physicochim. URSS. 1 (1934) 364–449.

[61] E.-.Z. El-Ashtoukhy, N.K. Amin, O. Abdelwahab, Removal of lead (II) and copper (II) from aqueous solution using pomegranate peel as a new adsorbent, Desalination. 223 (2008) 162–173.

[62] J.L. Sotelo, G. Ovejero, A. Rodríguez, S. Álvarez, J. García, Analysis and modeling of fixed bed column operations on flumequine removal onto activated carbon: pH influence and desorption studies, Chem. Eng. J. 228 (2013) 102–113.

[63] M. Kapur, M.K. Mondal, Competitive sorption of Cu(II) and Ni(II) ions from aqueous solutions: Kinetics, thermodynamics and desorption studies, J. Taiwan Inst. Chem. Eng. 45 (2014) 1803–1813.

[64] B.S. Liu, D.C. Tang, C.T. Au, Fabrication of analcime zeolite fibers by hydrothermal synthesis. Micropor. Mesorpor. Mat. 86 (2005) 145–151.

[65] H. Kurama, A. Zimmer, T. Reschetilowski, Chemical modification effect on the sorption capacities of natural clinoptilolite, Chem. Eng. Technol. 25 (2002) 301–305.

[66] G.E. Christidis, D. Moraetis, E. Keheyan, L. Akhalbedashvili, N. Kekelidze, R. Gevorkyan, H. Yeritsyan, H. Sargsyan, Chemical and thermal modification of natural HEU-type zeolitic materials from Armenia, Georgia and Greece, Appl. Clay Sci. 24 (2003) 79–91.

[67] H. Javadian, F. Ghorbani, H. Tayebi, S.H. Asl, Study of the adsorption of Cd (II) from aqueous solution using zeolite-based geopolymer, synthesized from coal fly ash; kinetic, isotherm and thermodynamic studies. Arabian J. Chem. 8 (2013) 837–849.

[68] A. Nezamzadeh-Ejhieh, A. Shirzadi Enhancement of the photocatalytic activity of Ferrous Oxide by doping onto the nano-clinoptilolite particles towards photodegradation of tetracycline, Chemosphere 107 (2014) 136–144.

[69] A. Bhatnagar, E. Kumar, M. Sillanpää, Nitrate removal from water by nano-alumina: Characterization and sorption studies, Chem. Eng. J. 163 (2010) 317–323.

[70] R. Katal, M.S. Baei, H.T. Rahmati, H. Esfandian, Kinetic, isotherm and thermodynamic study of nitrate adsorption from aqueous solution using modified rice husk, J. Ind. Eng. Chem. 18 (2012) 295–302.

[71] S.V. Dimitrova, D.R. Mehanjiev, Interaction of blast-furnace slag with heavy metal ions in water solutions. Water Res 34 (2000) 1957–1961.

[72] A. Shukla, Y.-H. Zhang, P. Dubey, The role of sawdust in the removal of unwanted materials from water. J. Hazard. Mat. B95 (2002) 137–152.

[73] M. Özacar, I.A. Şengil, Adsorption of metal complex dyes from aqueous solutions by pine sawdust. Biores. Technol. 96 (2005) 791–795.

[74] C. Namasivayam, D. Sangeetha, Application of coconut coir pith for the removal of sulfate and other anions from water. Desalination, 219 (2008) 1–13.

[75] C. Wu, C. Kuo, C. Lin, S. Lo, Modeling competitive adsorption of molybdate, sulfate, selenate, and selenite using a Freundlich-type multi-component isotherm, Chemosphere. 47 (2002) 283–292.

[76] C.K. Geethamani, S.T. Ramesh, R. Gandhimathi, P.V. Nidheesh, Alkali–treated fly ash for the removal of fluoride from aqueous solutions, Desalination and Water Treat. 52 (2014) 3466–3476.

[77] A. Moret, J. Rubio, Sulphate and molybdate ions uptake by chitin-based shrimp shells, Minerals Eng. 16 (2003) 715–722.

[78] H. Kalavathy, B. Karthik, L.R. Miranda, Removal and recovery of Ni and Zn from aqueous solution using activated carbon from Hevea brasiliensis: Batch and column studies, Colloids and Surfaces B: Biointerfaces. 78 (2010) 291–302.

[79] N.Y. Mezenner, A. Bensmaili, Kinetics and thermodynamic study of phosphate adsorption on iron hydroxide-eggshell waste, Chem. Eng. J. 147 (2009) 87–96.

[80] M.V. Subbaiah, Y.S. Yun, Biosorption of nickel(II) from aqueous solution by the fungal mat of trametes versicolor (Rainbow) biomass: equilibrium, kinetics, and thermodynamis studies, Biotechnol. Bioprocess Eng. 18 (2013) 280–288.

Supplementary Data

Figure 1. Different isotherms of SO_4^{2-} on Ba-modified analcime (ANA-Na-Ba) at a) 10 °C, b) 23 °C and c) 40 °C. Initial pH: 5–7, sorbent dosage: 5 g L^{-1}, contact time: 2 h.

Figure 2. Different isotherms of SO_4^{2-} on Ba-modified acid-washed analcime (ANA-Ac-Na-Ba) at a) 10 °C, b) 23 °C and c) 40 °C. Initial pH: 3–4, sorbent dosage: 5 g L^{-1}, contact time: 2 h.

Figure 3. Different isotherms of SO_4^{2-} on Ba-modified commercial zeolite (ZSM5-Na-Ba) at a) 10°C, b) 23°C and c) 40°C. Initial pH: 4–7, sorbent dosage: 5 g L^{-1}, contact time: 2 h.

Table 1. Isotherm constants of models applied for SO_4^{2-} removal on ANA-Na-Ba, ANA-Ac-Na-Ba, and ZSM5-Na-Ba.

Experimental/ Model	Constant [unit]	ANA-Na-Ba			ANA-Ac-Na-Ba			ZSM5-Na-Ba		
		10 °C	23 °C	40 °C	10 °C	23 °C	40 °C	10 °C	23 °C	40 °C
Experimental	q_m[mg g^{-1}]	1.582	2.344	6.918	12.049	13.696	13.516	2.884	3.766	5.725
Model										
Langmuir	q_m [mg g^{-1}]	2.434	2.736	15.401	11.348	10.887	11.841	3.525	4.205	6.160
	b_L [L mg^{-1}]	0.0062	0.009	0.001	2.153	1.399	2.040	0.014	0.022	0.024
	R^2	0.874	0.976	0.894	0.834	0.870	0.811	0.946	0.929	0.961
	RMSE	0.216	0.089	0.882	1.546	1.670	1.653	0.214	0.275	0.257
	χ^2	0.473	0.0004	2.484	5.069	2.097	4.603	0.247	0.185	0.162
Freundlich	K_F (mg g^{-1})	0.070	0.376	0.055	5.419	4.827	5.448	0.335	0.829	1.232
	$1/n_F$	0.546	0.283	0.759	0.140	0.169	0.156	0.374	0.254	0.259
	R^2	0.797	0.857	0.857	0.886	0.922	0.934	0.869	0.817	0.852
	RMSE	0.274	0.219	1.028	1.282	1.291	0.974	0.371	0.479	0.503
	χ^2	0.696	0.195	2.974	3.166	1.997	2.922	0.582	0.489	0.539

Experimental/ Model	Constant [unit]	ANA-Na-Ba			ANA-Ac-Na-Ba			ZSM5-Na-Ba		
		10 °C	23 °C	40 °C	10 °C	23 °C	40 °C	10 °C	23 °C	40 °C
Dubinin–Raduschkevich	q_m [mg g^{-1}]	1.638	2.233	6.960	11.707	12.241	12.392	2.661	3.644	5.144
	B [mol^2J^{-2}]	0.0007	0.0007	0.003	1.9E-5	1.8E-05	1.7E-05	0.0002	0.0002	0.0001
	R^2	0.975	0.908	0.982	0.604	0.592	0.505	0.942	0.989	0.983
	RMSE	0.096	0.176	0.368	2.389	2.959	2.677	0.222	0.118	0.401
	χ^2	1.269	0.195	2.122	2.259E+156	2.35E+147	2.668E+152	0.408	0.030	0.272
Temkin	b_T	3600	4434.095	852.540	2126.242	2044.069	2104.035	2864.316	3064.53	2069.908
	A_T [L g^{-1}]	0.045	0.110	0.016	161.059	56.698	107.057	0.110	0.294	0.324
	R^2	0.898	0.926	0.966	0.904	0.916	0.928	0.936	0.877	0.918
	RMSE	0.194	0.158	0.502	1.174	1.341	1.020	0.233	0.393	0.374
	χ^2	0.252	0.091	0.666	3.295	1.936	3.079	0.228	0.331	0.307
Bi-Langmuir	q_{m1}[mg g^{-1}]	2.436	1.367	7.051	8.515	7.246	7.837	1.762	2.103	3.080
	q_{m2}[mg g^{-1}]	3.634	1.369	8.344	3.781	8.267	7.815	1.762	2.103	3.080
	b_{L1}[L mg^{-1}]	0.006	0.009	0.001	0.066	0.005	4.591	0.014	0.022	0.024
	b_{L2}[L mg^{-1}]	0	0.009	0.001	1E30	2.736	0.007	0.014	0.022	0.024
	R^2	0.874	0.976	0.894	0.924	0.954	0.947	0.946	0.929	0.961
	RMSE	0.256	0.106	1.043	1.174	1.216	0.950	0.262	0.355	0.304
	χ^2	0.472	0.031	2.484	2.804	1.082	2.396	0.247	0.185	0.162
Sips	q_m [mg g^{-1}]	1.583	2.478	6.933	15.447	19.847	30.309	2.906	3.699	5.726
	b_S [L mg^{-1}]	0.013	0.011	0.005	0.147	0.021	9.22E-04	0.020	0.024	0.027
	n_S	3.186	1.393	2.779	0.321	0.289	0.217	1.674	2.102	1.300
	R^2	0.989	0.990	0.991	0.910	0.943	0.934	0.976	0.995	0.970

Experimental/ Model	Constant [unit]	ANA-Na-Ba			ANA-Ac-Na-Ba			ZSM5-Na-Ba		
		10 °C	23 °C	40 °C	10 °C	23 °C	40 °C	10 °C	23 °C	40 °C
	RMSE	0.070	0.061	0.277	1.201	1.216	1.014	0.157	0.080	0.247
	χ^2	0.105	0.015	0.166	3.262	1.660	2.997	0.082	0.009	0.108
Redlich–Peterson	K_R[L g^{-1}]	0.022	0.019	0.017	55.593	35.911	111.155	0.036	0.059	0.130
	a_R[L mg^{-1}]	5.00E-2	1.91E-3	3.93E-06	8.241	5.627	18.581	2.27E-3	2.64E-03	0.015
	B	0.730	1.189	1.823	0.900	0.883	0.862	1.251	1.273	1.053
	R^2	0.840	0.995	0.913	0.897	0.952	0.937	0.961	0.971	0.964
	RMSE	0.263	0.046	0.865	1.283	1.108	0.991	0.198	0.195	0.269
	χ^2	0.574	0.008	2.052	3.535	1.278	2.853	0.176	0.081	0.145
Toth	q_m[mg g^{-1}]	1.546	2.420	6.663	18.124	49.304	122.333	2.912	3.668	5.750
	K_{Th}[mg L^{-3}]Th	0.007	0.007	0.003	912.000	689411.2	3.58E+10	0.011	0.013	0.019
	Th	31.561	1.746	64.355	0.196	0.100	0.063	1.993	3.049	1.350
	R^2	0.961	0.993	0.950	0.908	0.939	0.935	0.966	0.987	0.967
	RMSE	0.130	0.053	0.653	1.214	1.251	1.010	0.186	0.132	0.258
	χ^2	0.211	0.012	1.702	3.290	1.697	2.983	0.148	0.036	0.126